Increasing superconducting transition temperature in MgB_2 by epitaxial tensile strain

A. V. Pogrebnyakov[*][†][‡], J. M. Redwing[†][‡], S. Raghavan[†][‡], V. Vaithyanathan[†][‡], D. G. Schlom[†][‡], S. Y. Xu[*][‡], Qi Li[*][‡], D. A. Tenne[*][‡], A. Soukiassian[†][‡], X. X. Xi[*][†][‡], M. D. Johannes[§], D. Kasinathan[§], W. E. Pickett[§], J. S. Wu[‖] & J. C. H. Spence[‖]

[*] *Department of Physics, The Pennsylvania State University, University Park, PA 16802*

[†] *Department of Materials Science and Engineering,*
The Pennsylvania State University, University Park, PA 16802

[‡] *Materials Research Institute, The Pennsylvania*
State University, University Park, PA 16802

[§] *Department of Physics, University of California, Davis, CA 95616 and*

[‖] *Department of Physics and Astronomy,*
Arizona State University, Tempe, AZ 85287

Since the discovery of superconductivity in MgB_2 by Nagamatsu *et al.* [1], many research groups have applied an exhaustive battery of techniques in an attempt to increase the transition temperature T_c, including substitution, disorder and pressure. All these efforts have failed, and the highest T_c in MgB_2 remains at about 40 K. Doping and chemical substitution in MgB_2 are difficult [2]. The few successful cases such as substitution of Mg by Al [3] and B with C [4] have so far always suppressed T_c. Although atomic disorder induced by proton irradiation enhances the pinning of vortices, it also reduces T_c [5]. Subjecting MgB_2 to pressure also causes T_c to decrease [6]. The few higher T_c values reported are from the ^{10}B isotope effect ($T_c = 40.2$ K) [7] and by Hur *et al.* when they exposed B crystals to Mg vapor ($T_c^{onset} = 41.7$ K and zero-resistance $T_{c0} = 39.8$ K) [8]. This situation calls into question whether and how the T_c of MgB_2 can be raised. Here we show a systematic increase of T_c with epitaxial tensile strain built into MgB_2 films well beyond the bulk value (the highest $T_{c0} = 41.8$ K). Further, we identify the underlying mechanism, among several materials characteristics that determine T_c, to be the softening of the E_{2g} phonon, a possible avenue to even higher T_c.

There are two new and remarkable features of MgB_2: its high value of T_c, almost twice as high as any other intermetallic material, and that it is a clear and rather extreme example of a "two gap" superconductor which have interested theorists for decades [9–11]. This two gap character arises due to two qualitatively different Fermi surfaces (called σ and π) and their different pairing strengths (extremely strong and weak, respectively). The σ contribution is dominant, however, and specifically the contribution from the B-B stretch modes (of E_{2g} symmetry) in the B_2 graphene layer [12, 13]. Since any significant change in T_c should arise from this dominant contribution, it suffices to consider only this contribution. According to the McMillan-Allen-Dynes expression,

$$T_c \propto \omega e^{-f(\lambda,\hat{\mu})}, \tag{1}$$

where ω is the phonon frequency, $f(\lambda,\hat{\mu}) = (1+\lambda)/(\lambda-\hat{\mu})$, and $\hat{\mu}$ is similar to the Coulomb repulsion μ^*. The electron-phonon coupling in a multiband superconductor is a matrix, but here we only consider the maximum element $\lambda^{\sigma\sigma}_{E_{2g}}$.

$$\lambda^{\sigma\sigma}_{E_{2g}} \propto \frac{m^*|\mathcal{D}|^2}{M\omega^2}, \tag{2}$$

where the σ band effective mass m^* is proportional to the density of states of holes in the σ band at the Fermi level, $\mathcal{D}$ is the deformation potential, and M is the B mass. A change in T_c can arise from any combination of changes in ω, λ, m^*, or $\hat{\mu}$. For example, the experimentally observed suppression of T_c by Al doping can be attributed to a decrease in the σ-band hole density of states [3], and the pressure effect attributed to a decrease in λ accompanied by an increase in the E_{2g} phonon frequency [14].

The epitaxial MgB_2 films in this work were deposited by a hybrid physical-chemical vapor deposition (HPCVD) technique [15]. Pure magnesium chips were heated simultaneously with the substrate to 720°C to generate a high Mg pressure, and 1000 ppm diborane (B_2H_6) in H_2 was used as the B precursor. The carrier gas was a H_2 flow of 450 sccm at a pressure of 100 Torr. The films were deposited on both (0001) 4H-SiC and (0001) sapphire substrates. We have shown previously that films on (0001) SiC are c-axis oriented and epitaxial with an in-plane alignment of the a-axis of MgB_2 with that of SiC [16]. Films on (0001) sapphire are also c-axis oriented and epitaxial, but the a-axis of MgB_2 is rotated by 30° in-plane from the a-axis of sapphire [15]. Because of the highly reducing H_2 ambient during the deposition and the high purity source of B from B_2H_6, the HPCVD technique produces very clean MgB_2 thin films with a residual resistivity at T_c as low as 0.26 $\mu\Omega$cm [17].

We have reported previously that the properties of MgB_2 films on (0001) SiC depend on film thickness [17]. We found that a similar dependence also exists for films on (0001) sapphire substrates. Figure 1(a) shows resistivity versus temperature curves for MgB_2 films with different thicknesses grown on sapphire substrates, and Fig. 1(b) shows the curves for films on SiC substrates. The figures clearly show that most samples here have T_{c0} above 40 K, considerably higher than that of the bulk MgB_2. Further, T_c becomes higher as the film thickness increases. The thickness dependence of the zero-resistance T_{c0} for both substrates is plotted in Fig. 1(c). A clear trend of increasing T_{c0} with film thickness is seen for both substrates with T_{c0} consistently 1 - 1.5 degree higher in films on SiC than on sapphire. The highest T_{c0} was observed in a 3400 Å thick MgB_2 film on a SiC substrate with $T_{c0} = 41.8$ K, about two degrees higher than all previously-reported values.

X-ray diffraction analysis shows a direct correlation between the lattice constants of the films, indicating biaxial strain, and T_{c0}. From $\theta - 2\theta$ scans we measured the c-axis lattice constants, and in conjunction with ϕ scans of asymmetric reflections we determined the a-axis lattice constants. Figure 2 shows (a) the a-axis and (b) the c-axis lattice constants of several $\mathrm{MgB_2}$ films of different thicknesses and different T_{c0}'s. Despite the large error bars, we clearly see that a higher T_{c0} corresponds to a larger a-axis lattice constant and a smaller c-axis lattice constant. More strikingly, although the results on SiC and sapphire follow two different T_{c0} versus thickness curves in Fig. 1(c), they fall on same T_{c0} versus lattice constant curves in Fig. 2, indicating that strain is the determining factor for T_{c0}. Compared to the bulk lattice constants of $a = 3.086$ Å and $c = 3.524$ Å [1], it is evident that the tensile strain in the films causes T_{c0} to increase beyond the bulk value, and the thicker the films the larger the tensile strain.

An increase of tensile strain with film thickness has been observed in films grown in the Volmer-Weber mode: film growth by initial nucleation of discrete islands which later coalesce [18, 19]. When the islands coalesce, they "zip up" because the surface energy of the islands is larger than the free energy of the grain boundaries, thus creating a tensile strain which increases with film thickness [20]. In the so-called "low-mobility" films, the height of the zipped boundary is less than the film thickness when the islands coalesce, and the "zipping-up" continues at the surface terrace level long afterwards [21]. Therefore, the tensile strain continues to increase with film thickness toward the upper bound value predicted by the Nix model [20]. The coalescence tensile strain has been suggested for GaN, a wide-band-gap compound semiconductor with a similar crystal structure to $\mathrm{MgB_2}$ [22]. Atomic force microscopy (AFM) images of two $\mathrm{MgB_2}$ films on SiC, one of 75 Å and the other of 900 Å, shown in Fig. 3(a) and 3(b), respectively, confirm that $\mathrm{MgB_2}$ films grow in the Volmer-Weber mode. Hexagonal-shaped $\mathrm{MgB_2}$ crystallites are seen in the thinner film, which coalesce into a continuous film at larger film thickness. The continued increase of tensile strain beyond coalescence and the surface terraces that are readily observable in thicker films indicate that $\mathrm{MgB_2}$ behaves like a low-mobility system at 720°C. This is consistent with the high melting temperature of B (2075°C) or $\mathrm{MgB_2}$ (it melts congruently at 2430 °C with pressure higher than 49000 Torr [23]). The grain growth as the film becomes thicker may also contribute to the tensile strain as the reduction of the defect density can generate a tensile strain in the film on the top [24]. Indeed the defect density is high near the $\mathrm{MgB_2}$/SiC substrate interface and decreases as the film thickness increases, as shown by the cross-sectional transmission electron microscopy (TEM) images in Fig. 3(c) (low magnification) and 3(d) (high resolution).

The magnitudes of the tensile strain are different on SiC and sapphire substrates, reflecting the differences in the lattice mismatch and thermal expansion mismatch. The in-plane lattice constant is $a = 3.07$ Å for 4H-SiC and $a = 4.765$ Å for sapphire, and thus the lattice mismatch could result in a much larger compressive strain for sapphire (11% compressive with the 30° in-plane rotation) than for SiC (0.1% compressive). The coefficient of thermal expansion at room temperature is 5.5×10^{-6} K^{-1} for MgB$_2$ [25], 3.0×10^{-6} K^{-1} for SiC [26], and 6.7×10^{-6} K^{-1} for sapphire [27]. Therefore, the thermal expansion mismatch will lead to a tensile strain in films on SiC, and a compressive strain in films on sapphire when the film is cooled from the deposition temperature. These factors are combined with the tensile growth strain to determine that there is a larger tensile strain in the MgB$_2$ films grown on SiC substrates.

The systematic increase of T_c with tensile strain shown in Fig. 2 allows us to investigate possible approaches to raise the T_c of MgB$_2$. For this purpose we have carried out first-principles calculations using the experimental lattice constants for the highest T_c sample in Fig. 2, which are $\Delta a/a = +0.55\%$ and $\Delta c/c = -0.25\%$. We found that this leads to a decrease in the σ hole concentration, $\Delta m^*/m^* = -1.2\%$, and $2\Delta|\mathcal{D}|/|\mathcal{D}| = -2.6\%$. The calculated change in the E_{2g} phonon frequency is in agreement with the experimentally extrapolated value from the polycrystalline sample of $\Delta\omega/\omega$= -5.5% [14]. From these values and using Eq. (2), we obtain

$$\frac{\Delta\lambda^{\sigma\sigma}_{E_{2g}}}{\lambda^{\sigma\sigma}_{E_{2g}}} = \frac{\Delta m^*}{m^*} + 2\frac{\Delta|\mathcal{D}|}{|\mathcal{D}|} - 2\frac{\Delta\omega}{\omega} = -1.2\% - 2.6\% + 11\% \approx +7\%. \tag{3}$$

From Eq. (1) and using as representative numbers, $\lambda = \lambda_\sigma + \lambda_\pi = 0.9 + 0.2 = 1.1$, and $\hat{\mu} = 0.2$:

$$\frac{\Delta T_c}{T_c} = \frac{\Delta\omega}{\omega} - \Delta f = \frac{\Delta\omega}{\omega} + \frac{1+\hat{\mu}}{(\lambda-\hat{\mu})^2}\Delta\lambda = -5.5\% + 10.4\% \approx +5\%. \tag{4}$$

This value is quite close to the experimental enhancement of T_c. This analysis identifies the underlying mechanism of the tensile-strain-induced increase in T_c as the softening of the E_{2g} bond-stretching mode. The decrease in the E_{2g} phonon frequency leads to the large relative increase in the σ band coupling strength (7%), which more than compensates the lowering of the temperature/energy scale governed by ω (and as mentioned, decreases by 5%). The result is also consistent with a previous first-principles calculation by Yildirim and Gülseren on the pressure effects in MgB$_2$ [28].

As a check on the validity of the theoretical calculations, we have measured the E_{2g} phonon frequencies of MgB$_2$ films of different thicknesses by Raman scattering. Raman spectra were taken using a SPEX Triplemate spectrometer in backscattering geometry with the 514.5 nm Ar$^+$ laser line as the excitation source. Figure 4 shows the spectra of two films: a 3400 Å-thick film on SiC and a 800 Å-thick film on sapphire. The thicker film on SiC has larger tensile strain than the thinner film on sapphire, and consequently has a higher T_{c0} as compared to the film on sapphire. The broad peak around 600 cm^{-1} has been assigned to the E_{2g} mode [14]. Although the peak is broad, a clear difference between the peak energies for the two films is seen. The higher T_c film on SiC has a softer E_{2g} mode than the lower T_c film on sapphire by about 20 cm^{-1}, i.e 3.3%.

There have been reports of reduced T_c in MgB$_2$ whereby a lower T_c corresponds to a higher E_{2g} phonon frequency [14, 29]. We show here that lowering the E_{2g} phonon frequency can increase T_c to above the bulk value. In our work, this was accomplished by the tensile strain built into the films during the HPCVD growth process, and the E_{2g} phonon softening is about 5.5%. An inspection of Eqns. (3) and (4) shows that if one can reduce the E_{2g} phonon frequency further, the T_c of MgB$_2$ will increase more than what we have shown here.

We gratefully acknowledge an extremely useful discussion with Bill Nix concerning the coalescence tensile strain. The work at Penn State is supported in part by ONR under grant Nos. N00014-00-1-0294 (Xi) and N0014-01-1-0006 (Redwing), by NSF under grant Nos. DMR-0306746 (Xi and Redwing), DMR-9876266 and DMR-9972973 (Li), and by DOE under grant Nos. DE-FG02-03ER46063 (Schlom) and DE-FG02-01ER45907 (Xi). The work at UC Davis is supported by NSF under grant No. DMR-0114818. The work at ASU is supported by NSF under grant No. DMR-0245702.

REFERENCES

[1] Nagamatsu, J., Nakagawa, N., Muranaka, T., Zenitani, Y. & Akimitsu, J. Superconductivity at 39 K in magnesium diboride. *Nature (London)* 410, 63–64 (2001).

[2] Cava, R. J., Zandbergen, H. W. & Inumaru, K. The substitutional chemistry of MgB_2. *Physica C* 385, 8–15 (2003).

[3] Slusky, J. S. *et al.*. Loss of superconductivity with the addition of Al to MgB_2 and a structural transition in $Mg_{1-x}Al_xB_2$. *Nature (London)* 410, 343–345 (2001).

[4] Lee, S., Masui, T., Yamamoto, A., Uchiyama, H. & Tajima, S. Carbon-substituted MgB_2 single crystals. *Physica C* 397, 7–13 (2003).

[5] Bugoslavsky, Y., Perkins, G. K., Qi, X., Cohen, L. F. & Caplin, A. D. Vortex dynamics in superconducting MgB_2 and prospects for applications. *Nature (London)* 410, 563–565 (2001).

[6] Monteverde, M. *et al.*. Pressure dependence of the superconducting transition temperature of magnesium diboride. *Science* 292, 75–77 (2001).

[7] Hinks, D. G., Claus, H. & Jorgensen, J. D. The complex nature of superconductivity in MgB_2 as revealed by the reduced total isotope effect. *Nature (London)* 411, 457–460 (2001).

[8] Hur, N. *et al.*. High-quality MgB_2 films on boron crystals with onset T_c of 41.7 K. *Appl. Phys. Lett.* 79, 4180–4182 (2001).

[9] Choi, H. J., Roundy, D., Sun, H., Cohen, M. L. & Louie, S. G. The origin of the anomalous superconducting properties of MgB_2. *Nature (London)* 418, 758–760 (2002).

[10] Pickett, W. Mind the double gap. *Nature (London)* 418, 733–734 (2002).

[11] Souma, S. *et al.*. The origin of multiple superconducting gaps in MgB_2. *Nature (London)* 423, 65–67 (2003).

[12] Liu, A. Y., Mazin, I. I. & Kortus, J. Beyond Eliashberg superconductivity in MgB_2 : Anharmonicity, two-phonon scattering, and multiple gaps. *Phys. Rev. Lett.* 87, 087005 (2001).

[13] An, J. M. & Pickett, W. E. Superconductivity of MgB_2: Covalent bonds driven metallic. *Phys. Rev. Lett.* 86, 4366–4369 (2001).

[14] Goncharov, A. F. & Struzhkin, V. V. Pressure dependence of the Raman spectrum, lattice parameters and superconducting critical temperature of MgB_2: evidence for pressure-driven phonon-assisted electronic topological transition. *Physica C* 385, 117–130 (2003).

[15] Zeng, X. H. *et al.*. *In situ* epitaxial MgB_2 thin films for superconducting electronics. *Nature Materials* 1, 35–38 (2002).

[16] Zeng, X. H. *et al.*. Superconducting MgB_2 thin films on silicon carbide substrates by hybrid physical-chemical vapor deposition. *Appl. Phys. Lett.* 82, 2097–2099 (2003).

[17] Pogrebnyakov, A. V. *et al.*. Thickness dependence of the properties of epitaxial MgB_2 thin films grown by hybrid physical-chemical vapor deposition. *Appl. Phys. Lett.* 82, 4319–4321 (2003).

[18] Floro, J. A., Chason, E., Cammarata, R. C. & Srolovitz, D. J. Physical origins of intrinsic stresses in Volmer-Weber thin films. *MRS Bulletin* 27(1), 19–25 (2002).

[19] Koch, R. The intrinsic stress of polycrystalline and epitaxial thin metal films. *J. Phys.: Condens. Matter* 6, 9519–9550 (1994).

[20] Nix, W. D. & Clemens, B. M. Crystallite coalescence: A mechanism for intrinsic tensile stresses in thin films. *J. Mater. Res.* 14, 3467–3473 (1999).

[21] Sheldon, B. W., Lau, K. H. A. & Rajamani, A. Intrinsic stress, island coalescence, and surface roughness during the growth of polycrystalline films. *J. Appl. Phys.* 90, 5097–5103 (2001).

[22] Etzkorn, E. V. & Clarke, D. R. Cracking of GaN films. *J. Appl. Phys.* 89, 1025–1034 (2001).

[23] Liu, Z. K., Schlom, D. G., Li, Q. & Xi, X. X. Thermodynamics of the Mg-B system: Implications for the deposition of MgB_2 thin films. *Appl. Phys. Lett.* 78, 3678–3680 (2001).

[24] Chaudhari, P. Grain growth and stress relief in thin films. *J. Vac. Sci. Technol.* 9, 520–522 (1972).

[25] Buzea, C. & Yamashita, T. Review of superconducting properties of MgB_2. *Supercond. Sci. Tech.* 14, R115–46 (2001).

[26] Li, Z. & Brandt, R. Thermal expansion of the hexagonal (6H) polytype of silicon carbide. *J. Amer. Chem. Soc.* 69, 863–866 (1986).

[27] Touloukian, Y. S., Kirby, R. K., Taylor, R. E. & Lee, T. Y. R. *Thermophysical Properties of Matter*, vol. 13 (Plenum, New York, 1977).

[28] Yildirim, T. & Gülseren, O. A simple theory of 40 K superconductivity in MgB_2: first-principles calculations of T_c, its dependence on boron mass and pressure. *J. Phys. Chem. Sol.* 63, 2201–2206 (2002).

[29] Masui, T., Lee, S. & Tajima, S. Carbon-substitution effect on the electronic properties of MgB_2 single crystals. *cond-mat/0312458* (2003).

FIGURE CAPTIONS

FIG. 1: Superconducting transition in MgB_2 films of different thicknesses. The resistivity versus temperature curves for films on (a) (0001) sapphire and (b) (0001) SiC substrates show that T_c increases and resistivity decreases as the film becomes thicker on both substrates. (c) Zero-resistance T_{c0} as a function of film thickness on both sapphire and SiC substrates. Similar increases with film thickness are seen for both substrates, although T_{c0} is one degree higher in films on SiC.

FIG. 2: Dependence of T_{c0} on film strain as determined by x-ray diffraction. (a) T_{c0} versus a-axis lattice constants. (b) T_{c0} versus c-axis lattice constants. The error bars indicate the accuracy of the measurement. The MgB_2 films on both sapphire and SiC substrates follow the same curves. Among data from the same substrate, a higher T_{c0} corresponds to a thicker film. As a comparison, the bulk lattice constants of MgB_2 are $a = 3.086$ Å and $c = 3.524$ Å.

FIG. 3: Growth mode and microstructure of MgB_2 films. (a) AFM image of a 75 Å-thick film. (b) AFM image of a 900 Å-thick film. Both films were grown on (0001) SiC substrates at 720°C with a B_2H_6 gas mixture flow rate of 50 sccm. Hexagonal-shaped MgB_2 crystallites seen in the thinner film coalesce into a continuous film at larger thickness. (c) Low-magnification and (d) high-resolution cross-section TEM images of a 2100 Å-thick MgB_2 film on (0001) SiC taken along the $[1\bar{1}00]$ direction. Both show that the defect density is high near the film/substrate interface and decreases as the film thickness increases. The dotted line in (d) indicates the MgB_2/SiC interface and the small arrows show the lattice deformation due to dislocations, most of which have Burgers vectors $\mathbf{b}$=[0001].

FIG. 4: Dependence of E_{2g} phonon frequency on film strain. The figure shows Raman spectra of two films: 3400 Å-thick on SiC and 800 Å-thick on sapphire. The thicker film on SiC has larger tensile strain and a higher T_{c0} than the thinner film on sapphire. The Raman result shows that the E_{2g} phonon in it has a lower frequency.

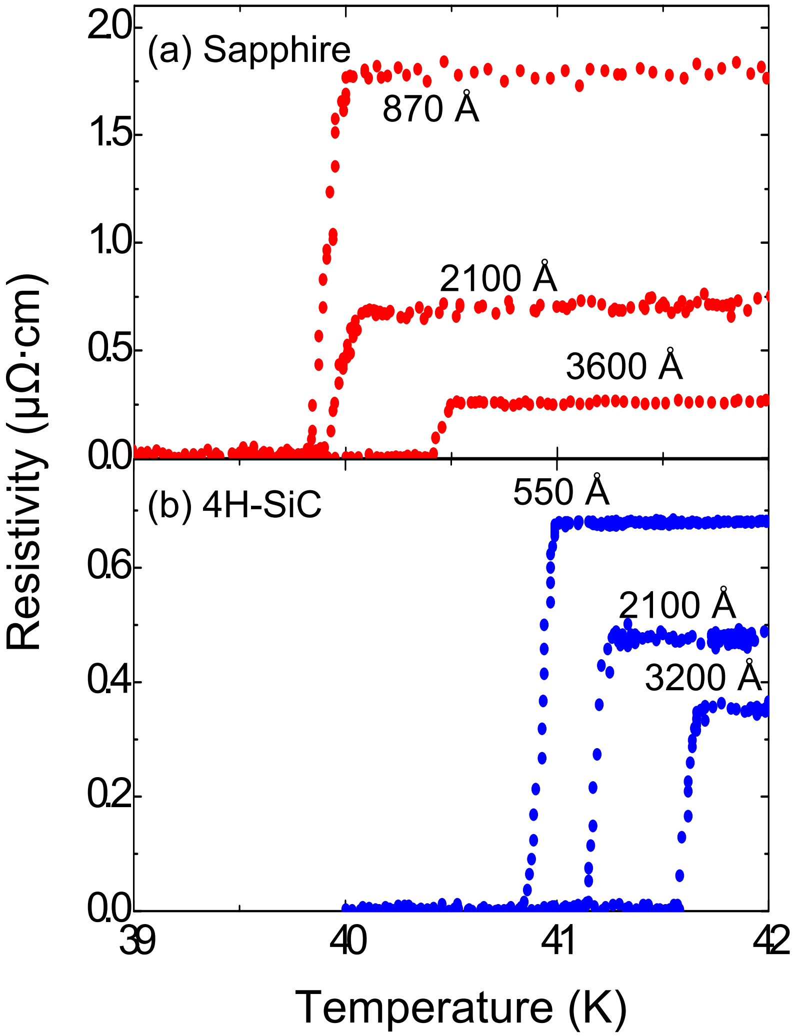

Fig. 1 (a) and (b)
Pogrebnyakov et al.

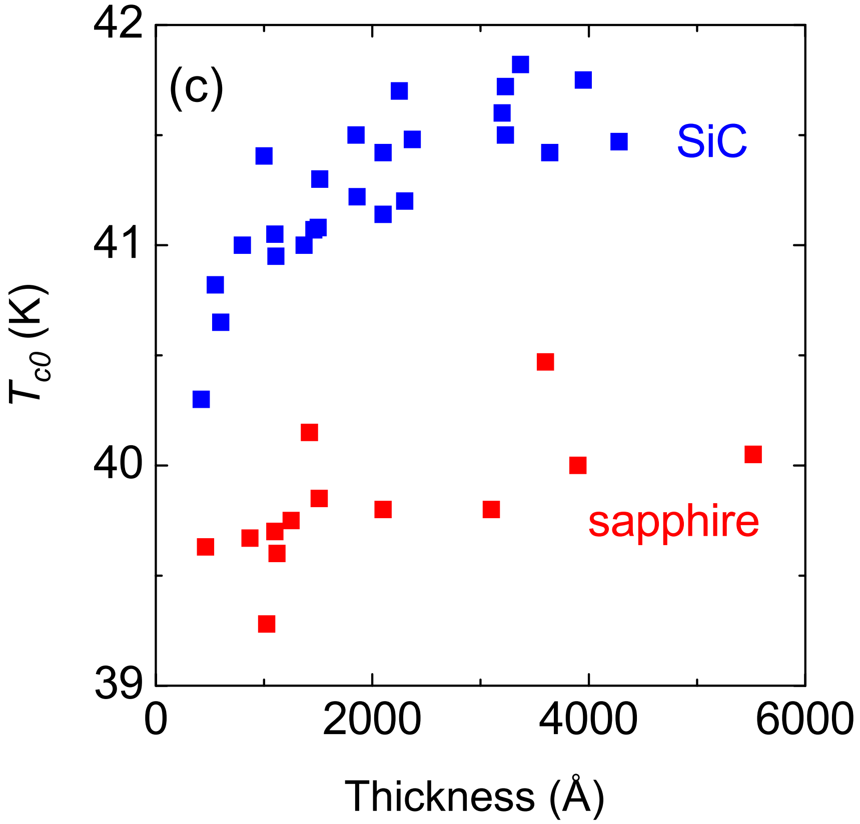

Fig. 1 (c)
Pogrebnyakov et al.

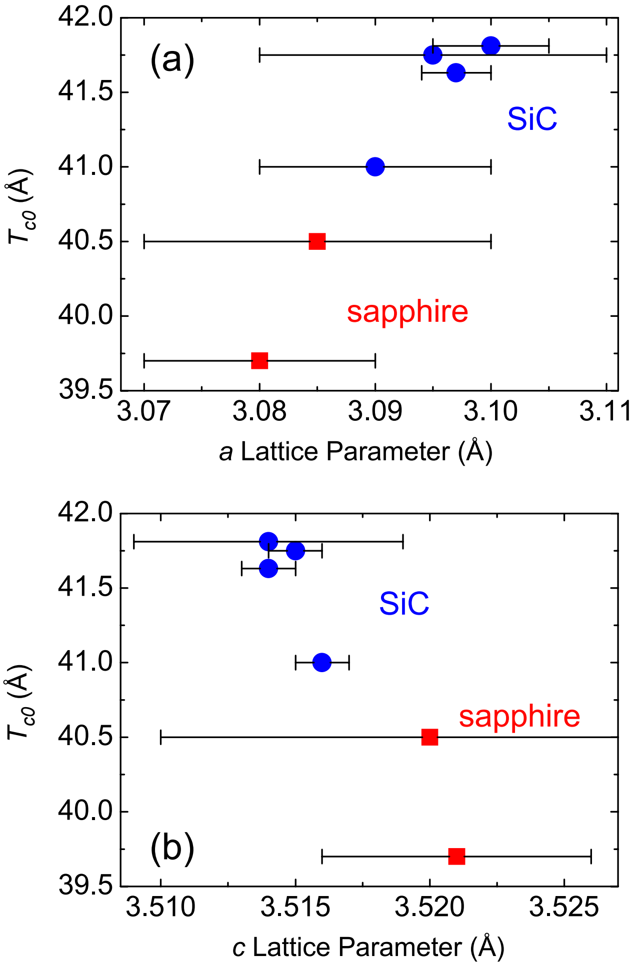

Fig. 2 (a) and (b)
Pogrebnyakov et al.

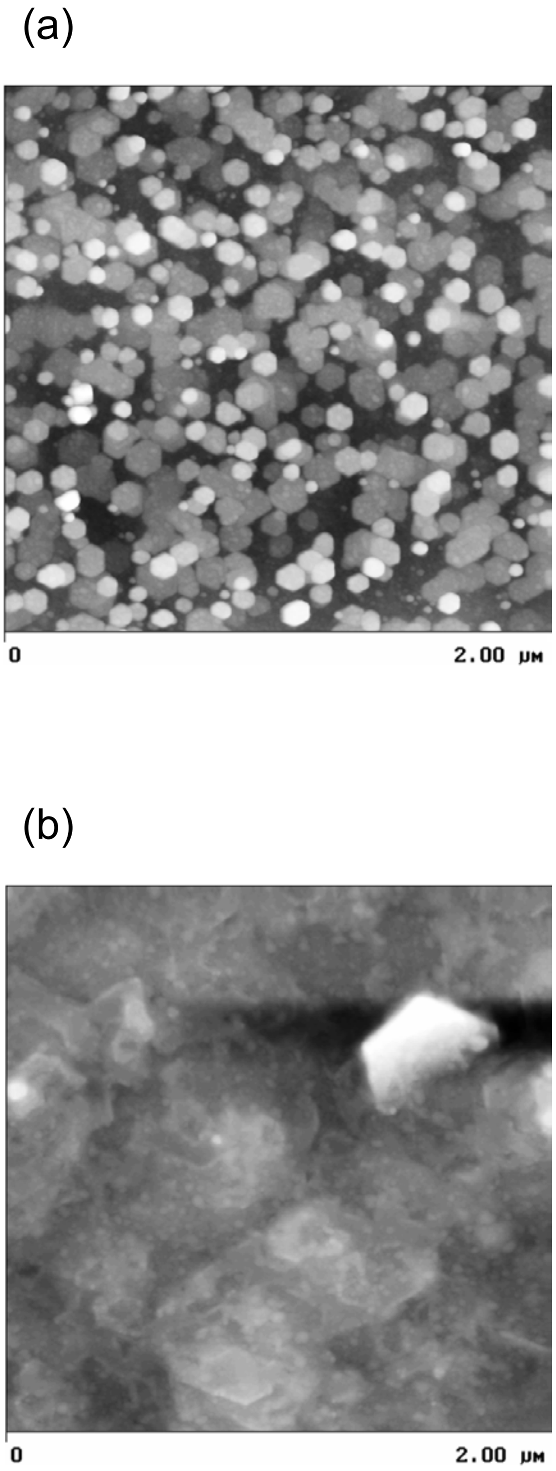

Fig. 3 (a) and (b)
Pogrebnyakov et al.

(c)

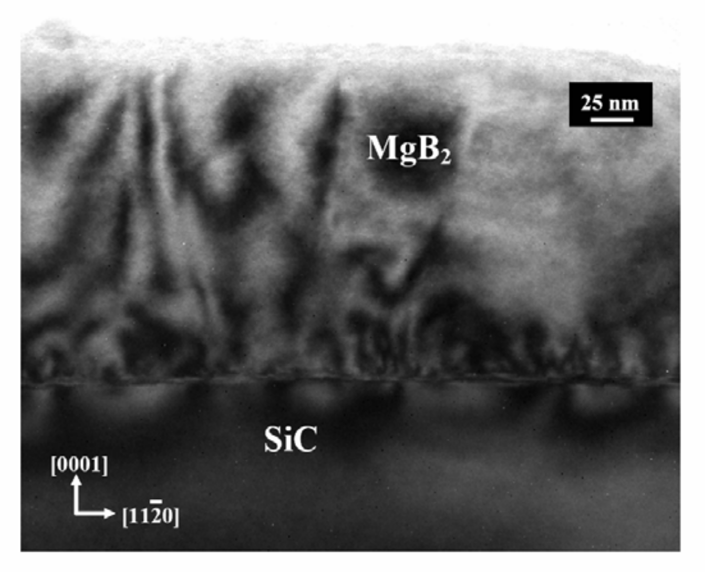

(d)

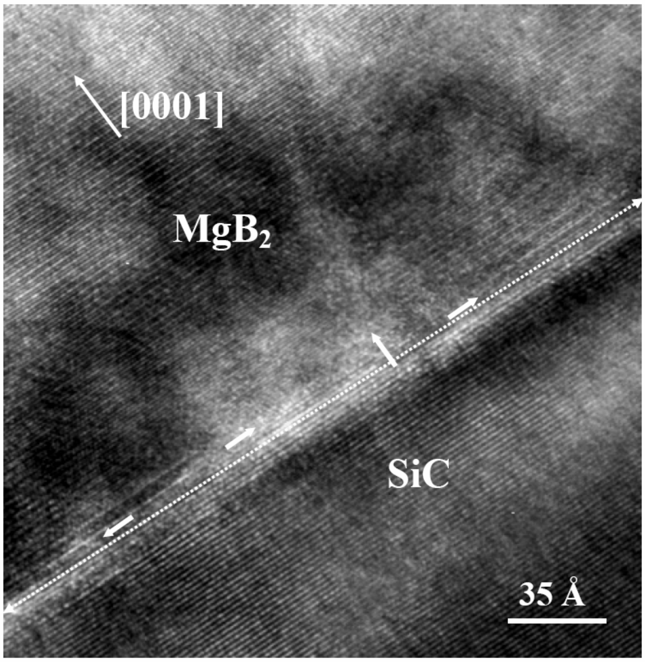

Fig. 3 (c) and (d)
Pogrebnyakov et al.

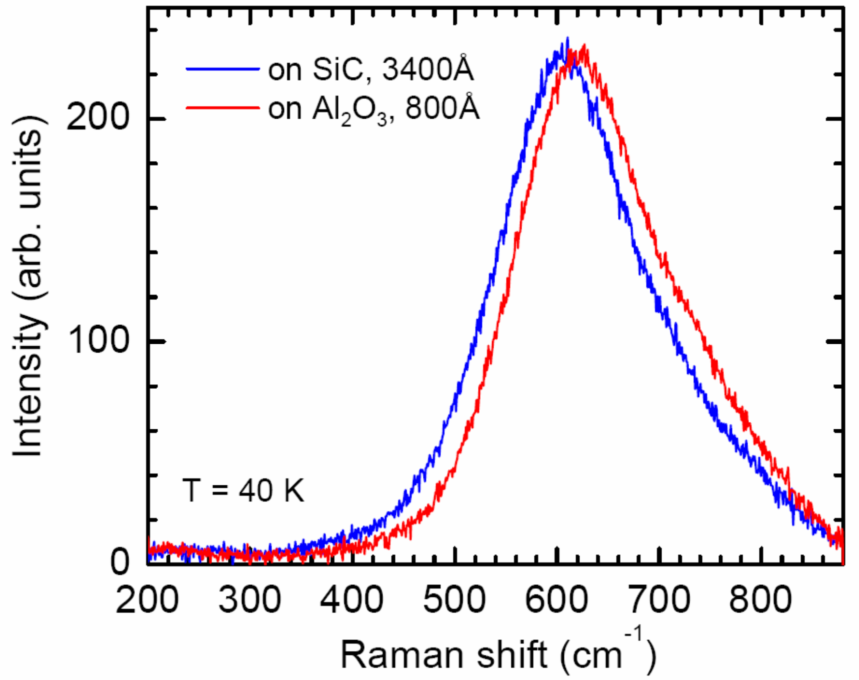

Fig. 4
Pogrebnyakov et al.